ADAMTS9 Regulates Skeletal Muscle Insulin Sensitivity Through Extracellular Matrix Alterations

Anne-Sofie Graae,[1] Niels Grarup,[2] Rasmus Ribel-Madsen,[2,3,4,5] Sara H. Lystbæk,[1] Trine Boesgaard,[2] Harald Staiger,[6,7,8] Andreas Fritsche,[6,7,9] Niels Wellner,[10] Karolina Sulek,[11] Mads Kjolby,[4,10] Marie Balslev Backe,[1] Sabina Chubanava,[11] Clara Prats,[12] Annette K. Serup,[13] Jesper B. Birk,[13] Johanne Dubail,[14] Linn Gillberg,[5] Sara G. Vienberg,[11] Anders Nykjær,[10] Bente Kiens,[13] Jørgen F.P. Wojtaszewski,[13] Steen Larsen,[12] Suneel S. Apte,[14] Hans-Ulrich Häring,[6,7,9] Allan Vaag,[15] Björn Zethelius,[16] Oluf Pedersen,[2] Jonas T. Treebak,[11] Torben Hansen,[2] and Birgitte Holst[1]

Diabetes 2019;68:502–514 | https://doi.org/10.2337/db18-0418

The *ADAMTS9* rs4607103 C allele is one of the few gene variants proposed to increase the risk of type 2 diabetes through an impairment of insulin sensitivity. We show that the variant is associated with increased expression of the secreted ADAMTS9 and decreased insulin sensitivity and signaling in human skeletal muscle. In line with this, mice lacking *Adamts9* selectively in skeletal muscle have improved insulin sensitivity. The molecular link between ADAMTS9 and insulin signaling was characterized further in a model where ADAMTS9 was overexpressed in skeletal muscle. This selective overexpression resulted in decreased insulin signaling presumably mediated through alterations of the integrin β1 signaling pathway and disruption of the intracellular cytoskeletal organization. Furthermore, this led to impaired mitochondrial function in mouse muscle—an observation found to be of translational character because humans carrying the *ADAMTS9* risk allele have decreased expression of mitochondrial markers. Finally, we found that the link between ADAMTS9 overexpression and impaired insulin signaling could be due to accumulation of harmful lipid intermediates. Our findings contribute to the understanding of the molecular mechanisms underlying insulin resistance and type 2 diabetes and point to inhibition of ADAMTS9 as a potential novel mode of treating insulin resistance.

Type 2 diabetes is determined by a complex interplay between environmental and genetic factors. Over the

[1]Section for Metabolic Receptology, Novo Nordisk Foundation Center for Basic Metabolic Research, Faculty of Health and Medical Sciences, University of Copenhagen, Copenhagen, Denmark
[2]Section for Metabolic Genetics, Novo Nordisk Foundation Center for Basic Metabolic Research, Faculty of Health and Medical Sciences, University of Copenhagen, Copenhagen, Denmark
[3]Department of Endocrinology, Rigshospitalet, Copenhagen, Denmark
[4]Danish Diabetes Academy, Novo Nordisk Foundation, Odense, Denmark
[5]Steno Diabetes Center, Gentofte, Denmark
[6]Institute for Diabetes Research and Metabolic Diseases, Helmholtz Centre Munich, University of Tübingen, Tübingen, Germany
[7]German Centre for Diabetes Research, Tübingen, Germany
[8]Institute of Pharmaceutical Sciences, Department of Pharmacy and Biochemistry, Eberhard Karls University Tübingen, Tübingen, Germany
[9]Department of Internal Medicine IV, University Hospital of Tübingen, Tübingen, Germany
[10]The Lundbeck Foundation Research Center MIND, Danish Research Institute of Translational Neuroscience, Nordic EMBL Partnership for Molecular Medicine, Department of Biomedicine, Aarhus University, Aarhus, Denmark
[11]Section for Integrative Physiology, Novo Nordisk Foundation Center for Basic Metabolic Research, Faculty of Health and Medical Sciences, University of Copenhagen, Copenhagen, Denmark
[12]Xlab, Center for Healthy Aging, Department of Biomedical Sciences, University of Copenhagen, Copenhagen, Denmark
[13]Section of Molecular Physiology, Department of Nutrition, Exercise and Sports, Faculty of Science, University of Copenhagen, Copenhagen, Denmark
[14]Department of Biomedical Engineering, Cleveland Clinic Lerner Research Institute, Cleveland, OH
[15]Cardiovascular and Metabolic Disease Translational Medicine Unit, Early Clinical Development, Innovative Medicines and Early Development Biotech Unit, AstraZeneca, Gothenburg, Sweden
[16]Geriatrics, Department of Public Health and Caring Services, Uppsala University, Uppsala, Sweden

Corresponding author: Birgitte Holst, holst@sund.ku.dk, Torben Hansen, torben.hansen@sund.ku.dk, or Jonas T. Treebak, jttreebak@sund.ku.dk

Received 30 April 2018 and accepted 14 December 2018

This article contains Supplementary Data online at http://diabetes.diabetesjournals.org/lookup/suppl/doi:10.2337/db18-0418/-/DC1.

A.-S.G., N.G., and R.R.-M. contributed equally to the manuscript.

J.T.T., T.H., and B.H. contributed equally to the manuscript.

past decade, genome-wide association studies have discovered more than 100 genetic variants that associate with type 2 diabetes (1). The majority of type 2 diabetes predisposition variants are related to pancreatic islet dysfunction (2). However, for most of these variants, the causal genes and the underlying biological processes leading to type 2 diabetes remain elusive (1). The rs4607103 C allele (frequency 76.2% in Europeans), located 38 kilobases upstream of the *ADAMTS9* (A disintegrin-like and metalloprotease with thrombospondin type I motif 9) gene (3,4), may be an exception, as the risk allele seems to associate with decreased insulin sensitivity in peripheral tissues rather than with β-cell dysfunction (4,5). However, whether *ADAMTS9* is the gene responsible for the association between the rs4607103 C allele and decreased insulin sensitivity has not been convincingly examined. In addition, the functional significance of ADAMTS9 for insulin action and glucose homeostasis has not been addressed previously.

ADAMTS9 is a secreted metalloprotease that is active against the large aggregating proteoglycans versican and aggrecan in the extracellular matrix (ECM) and other potential substrates that remain to be confirmed (6,7). Of note, a causal relationship between ECM alteration and insulin sensitivity in skeletal muscle has been suggested (8). For example, increased levels of ECM components have been observed in skeletal muscle of both obese humans and humans with type 2 diabetes (9) and in mice exposed to a high-fat diet (HFD) (10,11). Interventions that decrease the content of specific ECM components can prevent HFD-induced insulin resistance (10). In accordance with this, long-term treatment with a long-acting hyaluronidase increases insulin sensitivity in diet-induced obese mice (11). ECM alterations also can modify mitochondrial function, including respiration, which has been suggested to influence the pathogenesis of insulin resistance and type 2 diabetes (12,13). The heterodimeric integrin receptors are essential for this communication between the ECM and intracellular organization and function, which can act in a bidirectional manner. The integrins rely on recruitment of intracellular kinases, pseudokinases, and scaffolding proteins such as focal adhesion kinase (FAK) and integrin-linked kinase (ILK) for their signaling. Moreover, altered integrin receptor signaling and the resulting modulation of FAK and ILK have been shown to regulate insulin sensitivity in skeletal muscle, potentially through altered capillary density (10,14–17).

The aims of the current study were to determine whether *ADAMTS9* expression levels in humans are associated with the rs4607103 C allele and to characterize how ADAMTS9 modulates insulin action in both human and mouse models. We characterized the putative ADAMTS9-dependent insulin signaling pathway as well as the expression level of *ADAMTS9* in human skeletal muscle. A muscle-specific *Adamts9* knockout (KO) was developed to investigate the importance of ADAMTS9 for insulin sensitivity. In addition, *ADAMTS9* was overexpressed in mouse skeletal muscle to dissect the molecular mechanisms responsible for the modulation of insulin sensitivity. Using this method, we investigated the downstream insulin-mediated signaling pathways, ECM-mediated intracellular signaling, and skeletal muscle mitochondrial function. By using a catalytically impaired ADAMTS9, we were able to address the impact of proteolytic activity for the ADAMTS9-mediated changes in insulin action.

RESEARCH DESIGN AND METHODS

Human Studies

Study Populations

Study participants from six different study populations were included: Uppsala Longitudinal Study of Adult Men (ULSAM) (18), Danish young healthy individuals (19), Danish nondiabetic twin cohort (20), EUGENE2 (European Network on Functional Genomics of Type 2 Diabetes) (5), Danish family study (21), and a German study (Tübingen Family Study) (22). The study protocols were approved by the local ethics committees of the participating institutions and conducted in accordance with the principles of the Declaration of Helsinki.

Genotyping of rs4607103 was done by the KASPar SNP Genotyping System (KBiosciences, Hoddesdon, U.K.) or the GoldenGate Assay (Illumina, San Diego, CA). Additional details are available in the Supplementary Data.

Statistical Analysis

The analysis of insulin sensitivity in relation to the *ADAMTS9* rs4607103 genotype was done by linear regression or a linear mixed model adjusted for age and sex applying an additive genetic model. The M value, R_d value, and insulin sensitivity index were logarithmically transformed (base 10) before analysis. All data were standardized by conversion to *Z* scores. *Z* score–standardized effect size estimates and SEs were meta-analyzed by the RGui version 3.1.1 meta package using the inverse variance method. A mixed linear model that included family as a random factor was used to analyze *ADAMTS9* mRNA levels in skeletal muscle. A similar model was used in the twin population, with zygosity and pair number as random factors, to analyze insulin signaling proteins or mRNA levels of genes related to oxidative phosphorylation in skeletal muscle. $P < 0.05$ was considered significant. Additional details are available in the Supplementary Data.

Mouse Studies

Mouse Models

Male C57BL/6JBomTac mice (for in vivo gene electrotransfer), *Adamts9*-targeted mice with intragenic LacZ insertion (*Adamts9*$^{lacZ/+}$) (23), and *Adamts9*$^{fl/fl}$ mice with loxP sites inserted in introns 4 and 8 (24) crossed with mice carrying a Cre recombinase–encoding gene under the muscle-specific human α-skeletal actin (HSA) promoter (*Adamts9*$^{fl/fl}$ HSA-Cre) (25) were used. In vivo gene electrotransfer on 9-week-old mice was used to transfect tibialis anterior (TA) muscles as previously described (26). TA

muscles were dissected 7 days after transfection for subsequent ex vivo analyses. pCMV6-Entry plasmids containing Myc-DDK–tagged human ADAMTS9 (#RC217581; Origene) and pCMV6-Entry control plasmids (#PS100001; Origene) were used for studies that only compared ADAMTS9 overexpression with control plasmid in a paired setup. TA muscles expressing ADAMTS9 between 10-fold and 35-fold were used for further analysis. pcDNA3.1/Myc-His A plasmids (#V80020; Invitrogen) containing active human ADAMTS9 (wild-type [WT]-ADAMTS9) or catalytically mutated human ADAMTS9 (Glu435Ser) (mut-ADAMTS9) and pcDNA3.1/Myc-His A control plasmid were used for studies comparing WT-ADAMTS9 overexpression with mut-ADAMTS9 overexpression and control plasmid. All mouse experiments were performed in accordance with European directive 2010/63/EU of the European Parliament and the Council of the Protection of Animals Used for Scientific Purposes (Animal Experiments Inspectorate license nos. 2012-15-2934-307 and 2014-15-0201-00181). Additional details are available in the Supplementary Data.

Ex Vivo Studies

Western Blot Analysis. GAPDH was used as loading control. Control plasmid was set to 1, and all data were normalized to the corresponding control plasmid. Representative bands were chosen and are shown in the figures.

Quantitative PCR. Quantitative PCR was used to analyze cDNA or DNA purified from TA muscles. Expression levels were normalized to the average expression of the housekeeping genes TATA-box binding protein (TBP) for cDNA samples or average of nuclear DNA (nDNA) for DNA samples using the ΔΔCt method (27).

Energy Homeostasis. Analyses were performed as previously described and included glycogen quantification (26) and citrate synthase activity (28) assessed in pulverized TA muscles as well as mitochondrial respiration assessed in situ in saponin-permeabilized muscle fibers (29).

β-Galactosidase Staining and Immunohistochemistry. LacZ staining of *Adamts9*$^{lacZ/+}$ quadriceps muscles was followed by paraffin embedding (30). Muscle fibers were individually prepared and stained for mitochondrial networks (31).

Lipid Quantification. Intramyocellular triacylglycerol (TAG) was measured by a biochemical method in 1 mg of freeze-dried and dissected TA muscle (32). Diacylglycerol (DAG) isomers *sn*-1,2 and *sn*-1,3 content was analyzed in 1 mg freeze-dried and dissected TA muscle by thin-layer chromatography (33).

Metabolomics Analysis. Analysis was based on the principles previously described (34). Additional details are available in the Supplementary Data.

In Vivo Studies

An oral glucose tolerance test was carried out for in vivo characterization of *Adamts9*$^{fl/fl}$ HSA-Cre mice as previously described (35), and hyperinsulinemic-euglycemic clamp was based on principles previously described (36). Briefly, basal and insulin-stimulated glucose metabolism was determined in postabsorptive (overnight fasted 2200 h to 0900 h), body weight–matched anesthetized mice. Tissue-specific glucose uptake was determined in hyperinsulinemic-euglycemic state. In the basal period, the *Adamts9*$^{fl/fl}$ or *Adamts9*$^{fl/fl}$ HSA-Cre mice were infused with [^{3}H]glucose for 60 min to attain steady-state levels of [^{3}H]glucose in plasma and to determine endogenous glucose production. In the hyperinsulinemic-euglycemic clamp period, insulin was administered intravenously by a primed dose and by continuous (5 mU/kg/min) infusion to attain steady-state insulin levels together with [^{3}H]glucose for 90 min. A variable intravenous infusion of a glucose solution was used to maintain euglycemia as determined at 5-min intervals. For assessment of insulin-mediated glucose uptake in individual tissues, 2-deoxy-D-[^{14}C]glucose was administered as a bolus 30 min before the end of the experiment. Additional details are available in the Supplementary Data.

Statistical Analyses

Statistical significance was determined using GraphPad Prism 6 and 7 software by two-sided paired or unpaired one- or two-way ANOVA or Student *t* test as indicated. $P < 0.05$ was considered significant. The Prism outlier test was used to detect statistically significant outliers.

RESULTS

ADAMTS9 rs4607103 C Allele Is Associated With Decreased Insulin Sensitivity and Increased *ADAMTS9* Expression Levels in Skeletal Muscle of Humans

We combined previously published (5,18,19,22) and current data estimating insulin sensitivity from a hyperinsulinemic-euglycemic clamp with the insulin sensitivity index from a frequently sampled intravenous glucose tolerance test in a meta-analysis of 2,623 individuals of European origin. We found a significant association between the rs4607103 C allele and decreased insulin sensitivity (Fig. 1*A*).

ADAMTS9 is known to be highly expressed in human skeletal muscle (6), and we therefore investigated and found that the rs4607103 C risk allele is associated with higher *ADAMTS9* expression in human skeletal muscle compared with the protective T allele in individuals without diabetes (Fig. 1*B* and Supplementary Table 1). In skeletal muscle from twins without diabetes (Supplementary Table 2 and Supplementary Fig. 3), the C risk allele was associated with significantly lower Akt T308 phosphorylation (Fig. 1*C* and Supplementary Table 3) and a trend toward lower glycogen synthase activity (Fig. 1*D* and Supplementary Table 3).

Muscle-Specific *Adamts9* KO Mice Have Increased Insulin Sensitivity

To investigate the role of ADAMTS9 in glucose homeostasis in vivo, we developed *Adamts9*$^{fl/fl}$ HSA-Cre (muscle-specific *Adamts9* KO mice) because whole-body *Adamts9*

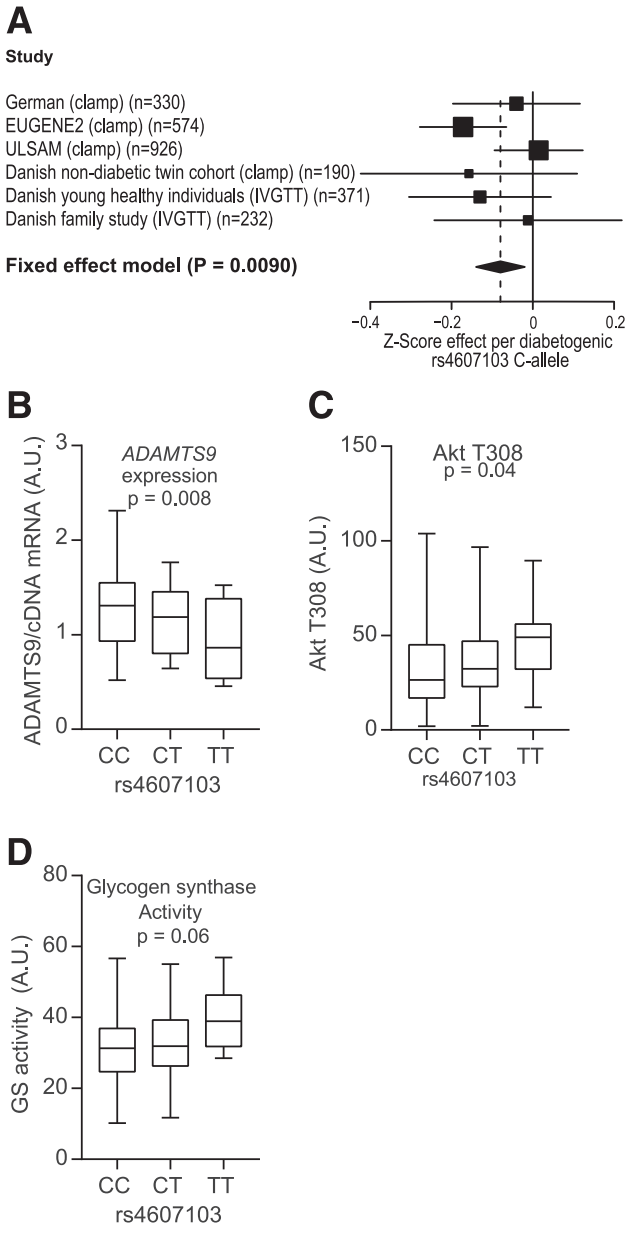

Figure 1—*ADAMTS9* rs4607103 is associated with decreased insulin sensitivity, differential *ADAMTS9* expression, and insulin signaling. *A*: Meta-analysis of estimates of insulin sensitivity (fixed-effects model: β = −0.080 standard deviation [95% CI −0.14 to −0.020]; *P* = 0.0090). *B*: *ADAMTS9* mRNA expression by quantitative PCR in the Danish Family Study (first-degree relatives of patients with type 2 diabetes) divided by genotype (CC *n* = 45, CT *n* = 31, TT *n* = 4; *P* = 0.008). *C* and *D*: C allele = rs4607103 risk allele; T allele = other allele. Danish nondiabetic twin cohort divided into genotypes (CC *n* = 108, CT *n* = 67, TT *n* = 7) after insulin stimulation. Akt Thr308 phosphorylation (*P* = 0.04) (*C*) and glycogen synthase (GS) activity (*P* = 0.06) (*D*) are shown. A mixed linear model was used assuming an additive genetic effect. *P* values are adjusted for sex, age, BMI, and family relationship. See also Supplementary Tables 1–3. A.U., arbitrary units; IVGTT, intravenous glucose tolerance test.

KO mice die at the onset of gastrulation (37). LacZ reporter under the control of the *Adamts9* promoter identified expression in skeletal muscles and endothelial cells (23) (Fig. 2*A*). Because of the high expression of *Adamts9* in endothelial cells, a complete deletion of *Adamts9* in muscle tissue was not possible (Fig. 2*B*). On chow diet (0 weeks of high-fat, high sucrose [HFHS] diet), no significant differences were observed between muscle-specific *Adamts9* KO mice and their WT littermates with regard to body weight and body composition (Fig. 2*C–E*) or glucose metabolism and insulin secretion (Supplementary Fig. 1*A* and *B*). Feeding with an HFHS diet for 22 weeks did not significantly change body weight or composition between the two groups (Fig. 2*C–E*). The muscle-specific *Adamts9* KO mice, however, did have significantly lower fasting plasma insulin levels than their littermate controls without affecting plasma glucose (Fig. 2*F* and *G*), suggesting that muscle-specific *Adamts9* KO mice are more insulin sensitive than their littermate controls. Insulin sensitivity, therefore, was examined by a hyperinsulinemic-euglycemic clamp. Muscle-specific *Adamts9* KO mice had a higher glucose infusion rate (GIR) (Fig. 2*H* and *I*), supporting the hypothesis of improved insulin sensitivity in mice lacking *Adamts9* in skeletal muscle. The increased GIR was due to an elevated whole-body R_d, whereas the endogenous glucose production was unaltered between genotypes, suggesting the effect to be independent of the liver (Fig. 2*J* and *K*). We also observed an increased glucose uptake in gastrocnemius skeletal muscle of muscle-specific *Adamts9* KO mice compared with littermate controls (Fig. 2*L*). Thus, the data from muscle-specific *Adamts9* KO mice are in line with data from humans showing that elevated levels of ADAMTS9 may contribute to modulation of insulin sensitivity in skeletal muscle.

ADAMTS9 Overexpression in Mouse Skeletal Muscle Attenuates Insulin Signaling

To understand the molecular determinant for the altered glucose homeostasis and to imitate the human condition in carriers of the rs4607103 C risk allele, we overexpressed *ADAMTS9* in mouse TA muscle by gene electrotransfer in a paired setup with an empty vector control (Supplementary Fig. 2*A*). This model is more suitable than a regular knock-in model because the specific single nucleotide polymorphism is not located in the coding region of the *ADAMTS9* gene. Activity of the overexpressed ADAMTS9 was assessed by the capacity to cleave the substrate versican (Supplementary Fig. 2*B*), since no specific antibody is described for ADAMTS9. Seven days after electroporation, we challenged the mice with a high dose of insulin and analyzed muscles 5 and 25 min after insulin injection. We observed a general attenuation of the insulin signaling pathway in muscles overexpressing ADAMTS9 under both basal and insulin-stimulated conditions. Both the protein level of the insulin receptor (IR) and the phosphorylation state of IR Y1150/1151 and IRS1 Y612 were decreased upon ADAMTS9 overexpression, independent of insulin (Fig. 3*A* and Supplementary Fig. 2*C*). The effect on IR seemed to be due to a decrease in the gene expression (Supplementary Fig. 3*D*). In addition, we found phosphorylation of Akt T308 and S473 relative to total

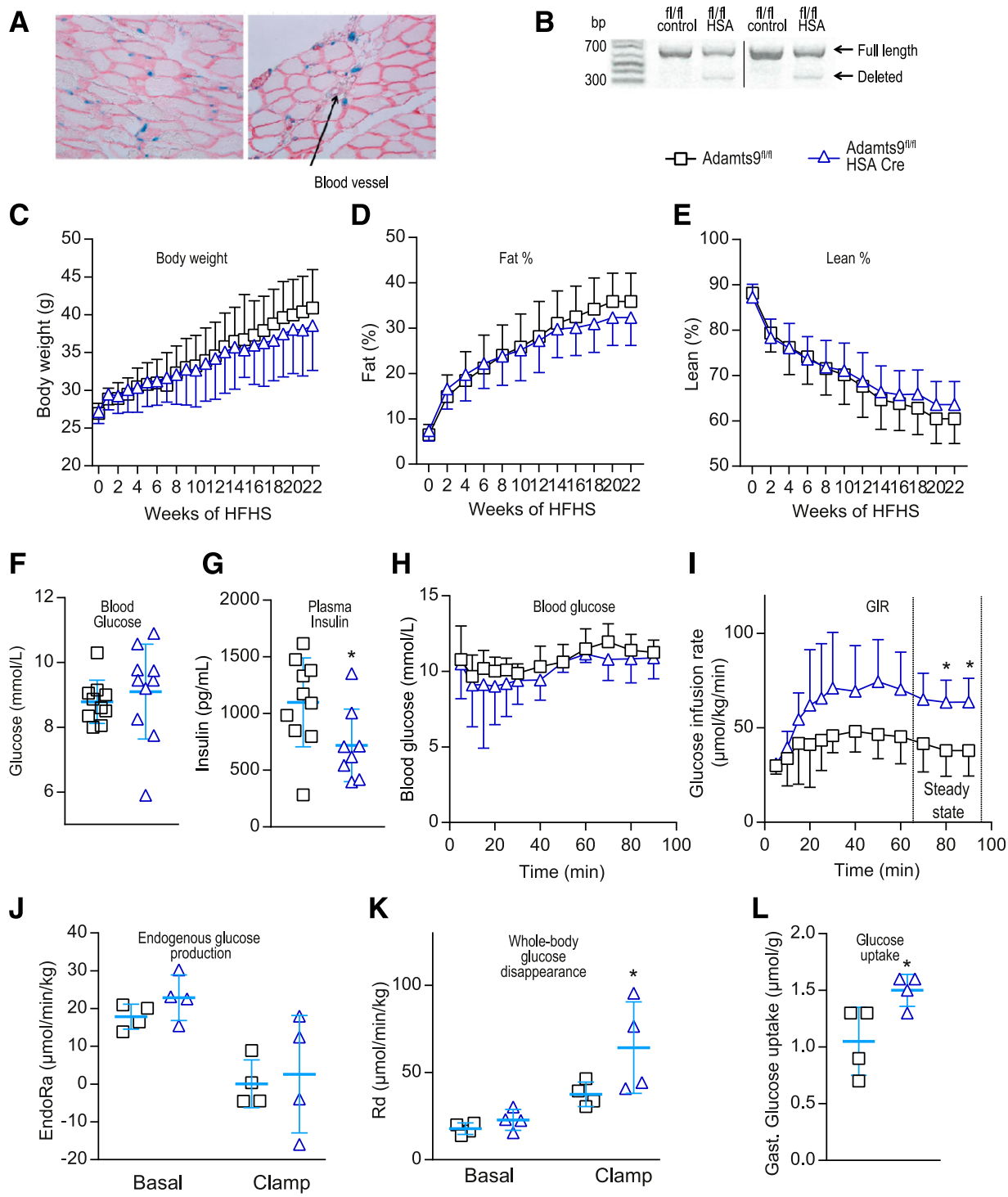

Figure 2—Muscle-specific *Adamts9* KO mice have increased insulin sensitivity. *A*: β-Galactosidase staining (blue) of *Adamts9*$^{lacZ/+}$ mouse skeletal muscle with laminin immunostaining (red). The arrow indicates a blood vessel. *B*: PCR verification of *Adamts9*$^{fl/fl}$ HSA-Cre mouse skeletal muscle cDNA (357-base pair [bp] band = floxed region is deleted; 704-bp band = full-length region). Dividing lines have been used in representative blots. *C–L*: Metabolic measurements and hyperinsulinemic-euglycemic clamp on *Adamts9*$^{fl/fl}$ and *Adamts9*$^{fl/fl}$ HSA-Cre (muscle-specific *Adamts9* KO) mice on an HFHS diet. Body weight (*C*), percent fat (fat %) (*D*), and percent lean (lean %) (*E*) are shown for the 22-week period of the HFHS diet from 15 weeks of age (n = 12 for *Adamts9*$^{fl/fl}$ until week 16 [thereafter, n = 11], n = 10 for *Adamts9*$^{fl/fl}$ HSA-Cre). Four-hour fasting blood glucose (n = 11 for *Adamts9*$^{fl/fl}$, n = 10 for *Adamts9*$^{fl/fl}$ HSA-Cre) (*F*) and plasma insulin (n = 10 for *Adamts9*$^{fl/fl}$, n = 8 for *Adamts9*$^{fl/fl}$ HSA-Cre) (*G*) are shown after 22 weeks on the HFHS diet at 37 weeks of age. *H–L*: Measures of hyperinsulinemic-euglycemic clamp after 22 weeks on the HFHS diet at 37 weeks of age (n = 4 in each group) including blood glucose (*H*), GIR (*I*), endogenous glucose production (EndoRa) (*J*), whole-body R_d during the clamp (*K*), and glucose uptake into gastrocnemius (Gast.) skeletal muscle (*L*). Data are mean ± SD. Statistical significance was determined using Student t test (*F*, *G*, *I*, and *L*) or two-way ANOVA with Sidak test for multiple comparisons (*J* and *K*). *$P < 0.05$ for effect of *Adamts9*$^{fl/fl}$ vs. *Adamts9*$^{fl/fl}$ HSA-Cre.

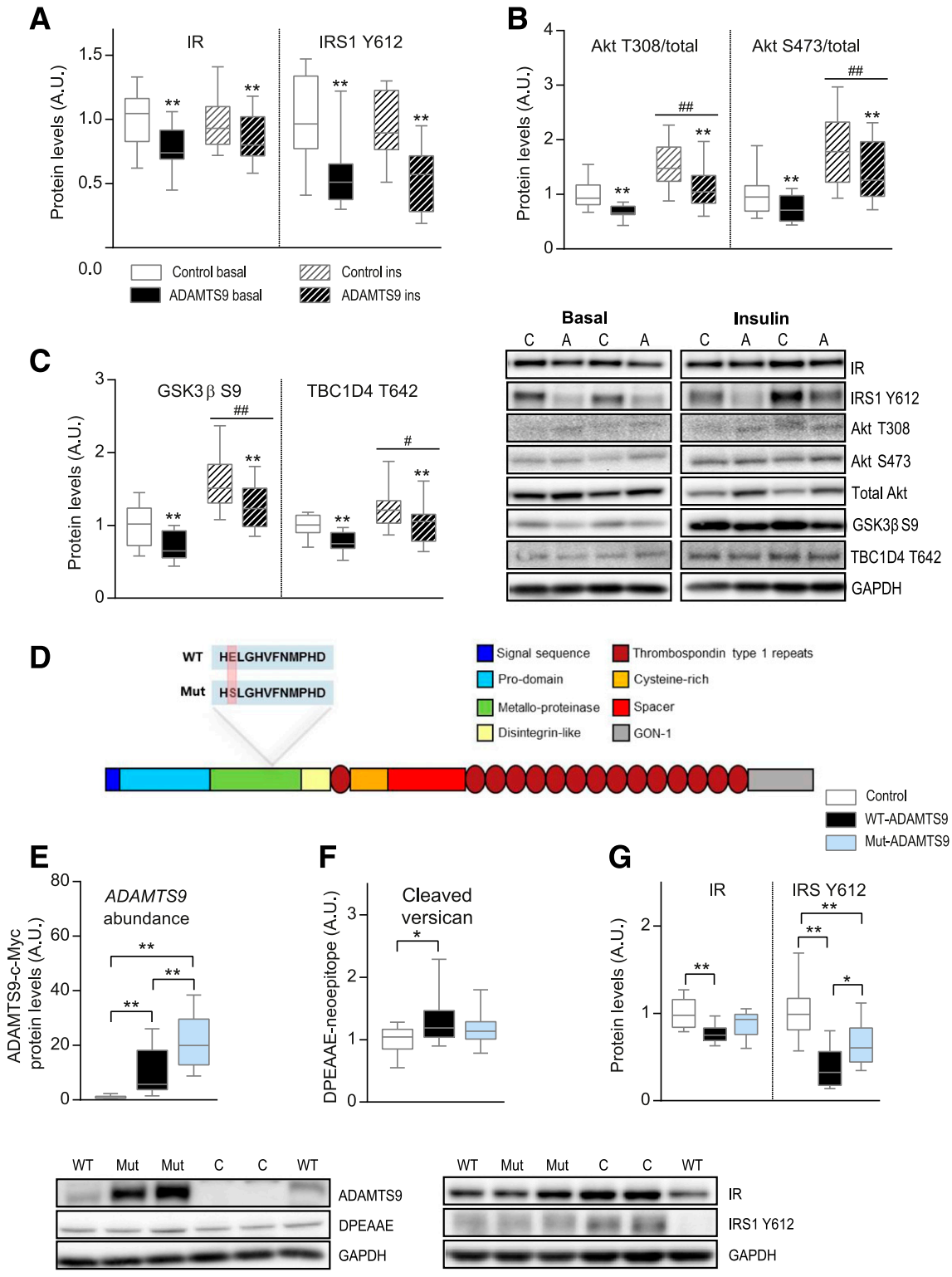

Figure 3—ADAMTS9 overexpression in mouse skeletal muscle decreases insulin (ins) signaling dependent on catalytic activity. *A–C*: Mice overexpressing ADAMTS9 or control plasmid in TA muscles were stimulated with either saline (basal) or 0.5 units/kg insulin for 25 min at 10 weeks of age. TA muscles were isolated and used for Western blot analyses (*A* and *C*: $n = 12$ for each group; *B*: saline samples for both groups $n = 10$; ins samples for both groups $n = 12$; results replicated twice and then pooled). Statistical significance was determined using paired two-way ANOVA with Sidak test for multiple comparisons. $^{**}P < 0.01$ for effect of ADAMTS9 overexpression vs. control plasmid; $\#P < 0.05$, $\#\#P < 0.01$ for main effect of ins vs. basal treatment. *D*: Schematic of ADAMTS9 and the location of the mutation to create mut-ADAMTS9. Catalytic site at amino acids 434–444 (HELGHVFNMPHD in WT-ADAMTS9; HSLGHVFNMPHD in mut-ADAMTS9). *E–G*: TA muscles overexpressing WT-ADAMTS9, mut-ADAMTS9, or control plasmid were used for Western blot analysis at 10 weeks of age (*E*: $n = 14$ for each group; *F* and *G*: $n = 13$ for WT-ADAMTS9 and control groups, $n = 14$ for mut-ADAMTS9; results replicated twice and then pooled).

Akt levels to be decreased in muscles overexpressing ADAMTS9 (Fig. 3*B*) as a result of upregulation of total Akt levels (Supplementary Fig. 2*E*). To test how ADAMTS9 overexpression influenced the function of Akt, we determined the phosphorylation states of two downstream Akt substrates, GSK-3β S9 and TBC1D4 T642, both of which were decreased upon ADAMTS9 overexpression compared with control at both basal and insulin-stimulated conditions (Fig. 3*C* and Supplementary Fig. 2*F*). These data suggest that the activity of Akt and other key enzymes in the insulin signaling pathway is diminished in muscles overexpressing ADAMTS9.

In view of the role of ADAMTS9 as an ECM-degrading enzyme, we examined whether the observed effects on insulin signaling are mediated through the catalytic activity of ADAMTS9. ADAMTS9 with a defective enzymatic activity (mut-ADAMTS9) (Fig. 3*D*) was overexpressed in mouse TA muscle in parallel with WT-ADAMTS9 and control plasmid. Of note, the mut-ADAMTS9 reached a higher protein level than the WT-ADAMTS9 potentially because of autocatalytic loss of WT-ADAMTS9, a known phenomenon in ADAMTS proteases (38) (Fig. 3*E*). The catalytic activity of the mut-ADAMTS9 was not completely abolished, as cleavage of the known ADAMTS9 substrate versican (DPEAAE-neoepitope) was only partly reduced compared with WT-ADAMTS9 (Fig. 3*F*), which also may result from coincident expression of other versican-degrading ADAMTS proteases (39). Despite higher levels of mut-ADAMTS9, the impairment of the insulin signaling pathway was not as pronounced as for WT-ADAMTS9 (Fig. 3*G* and Supplementary Fig. 2*G* and *H*). These results suggest, therefore, that the catalytic activity and, consequently, the cleavage of substrates in the ECM are at least partly responsible for the observed effects of ADAMTS9 on insulin signaling.

ADAMTS9 Overexpression in Mouse Skeletal Muscle Alters Integrin Signaling and Modulates the Cytoskeleton and Capillary Density

Because ECM is communicating with the cell through integrin receptors, we investigated whether integrin signaling was altered by ADAMTS9 overexpression. The integrin β1 receptor was strongly upregulated when overexpressing WT-ADAMTS9 (Fig. 4*A*), possibly to compensate for the decreased ECM attachment upon cleavage by ADAMTS9 (40). This effect was completely abolished when the catalytically defective mut-ADAMTS9 was expressed. The overall levels of the downstream pseudokinase ILK and the adaptor protein PINCH were increased, whereas the activity of the downstream integrin signaling kinase FAK was decreased when measured by Y397 FAK phosphorylation (Fig. 4*B*). Both ILK and FAK have been shown previously to modulate vascularization; therefore, we measured the endothelial marker caveolin (41). Indeed, overexpression of ADAMTS9 in mouse TA muscle was found to decrease the level of caveolin (Fig. 4*C*), indicating a decreased capillary density.

Integrin receptor signaling modulates the cytoskeleton, which is the network supporting and organizing vesicles and organelles inside the cell. The mRNA expression level of desmin and myosin heavy chain 2 (*MYH2*), two constituents of the cytoskeleton in skeletal muscle, were downregulated when overexpressing WT-ADAMTS9 (Fig. 4*D*). Overall, overexpression of mut-ADAMTS9 induced a less pronounced phenotype than overexpression of the WT-ADAMTS9 in accordance with our previously obtained results. Desmin is an intermediate filament that plays an important role in the maintenance of cellular integrity of muscles, including organization of mitochondria. In both human diseases and mouse models, desmin deficiency negatively affects mitochondrial function (42). Therefore, we investigated whether mitochondrial function was altered after ADAMTS9 overexpression.

Overexpression of ADAMTS9 Decreases Mitochondrial Function and Content

Mitochondrial respiration analyses showed that muscle overexpressing ADAMTS9 had a generally lower respiration than controls after adding substrates, which activates complex I (CI), CII, and CIV (Fig. 5*A* and Supplementary Fig. 3*A*), independent of normalization to citrate synthase activity (Fig. 5). Reduced mitochondrial respiration may be explained by lower mitochondrial content. Indeed, we found that muscle overexpressing WT-ADAMTS9 had lower levels of the four mitochondrial complexes (CI–CIV) and the ATP synthase at both mRNA and protein levels (Fig. 5*B* and Supplementary Fig 3*B* and *C*) and diminished mitochondrial density as measured by citrate synthase activity and the ratio between mitochondrial DNA and nDNA (Fig. 5*C* and Supplementary Fig. 3*D*). Furthermore, expression levels of genes involved in mitochondrial biogenesis, including *PGC-1α*, *PGC-1β*, and *TFAM*, and genes involved in fission/fusion events, including *Mfn2* and *Dnm1l*, were decreased after ADAMTS9 overexpression (Fig. 5*D* and Supplementary Fig. 3*E*). In addition, the mitochondrial network was more fragmented in muscle overexpressing ADAMTS9 compared with control muscle (Supplementary Fig. 3*F*). This effect was partly reverted by use of the catalytically impaired mut-ADAMTS9 (Fig. 5*E*). The catalytic activity of ADAMTS9

E: The expression level of ADAMTS9 was estimated on the basis of a c-Myc tag on the WT-ADAMTS9 construct and the mut-ADAMTS9, whereas empty vector–transfected muscles reflect the background level. Statistical significance was determined using one-way ANOVA with Tukey test for multiple comparisons. $^{*}P < 0.05$, $^{**}P < 0.01$ for genotype effect (WT-ADAMTS9 vs. mut-ADAMTS9 vs. control). A.U., arbitrary units.

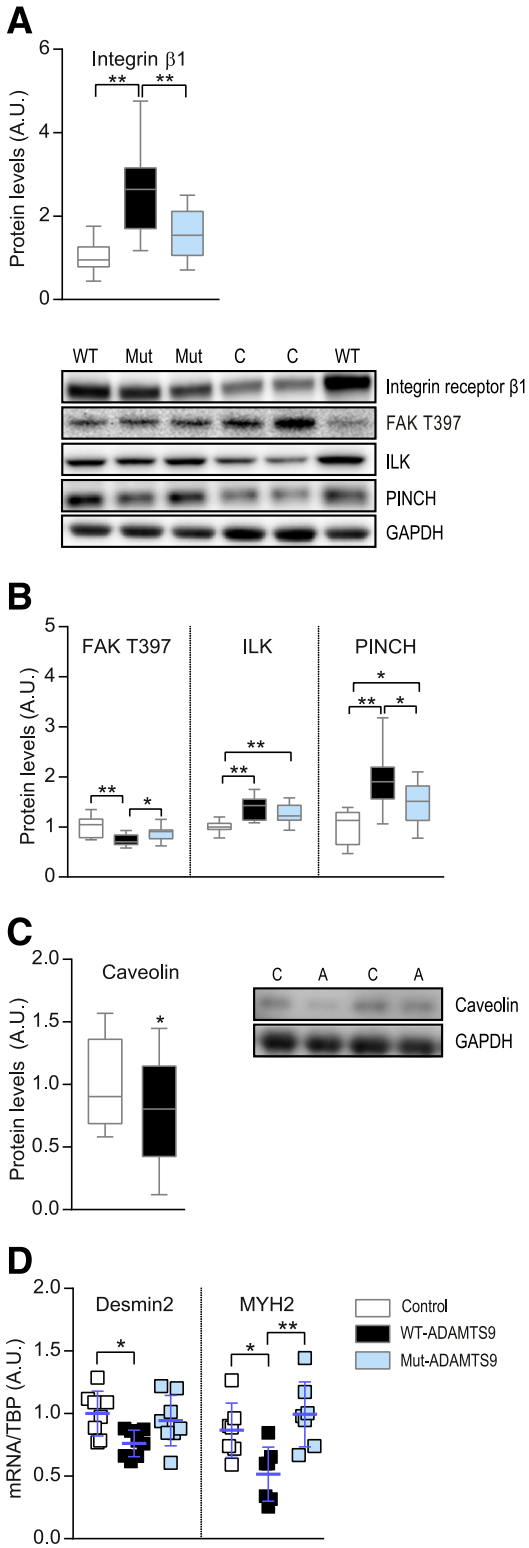

Figure 4—ADAMTS9 overexpression modulates integrin signaling, cytoskeletal proteins, and capillary density. *A*, *B*, and *D*: Mouse TA muscles overexpressing WT-ADAMTS9, mut-ADAMTS9, or control plasmid were isolated at 10 weeks of age and used for Western blot analyses (n = 13 for WT-ADAMTS9 and control groups [n = 11 for control group for PINCH], n = 14 for mut-ADAMTS9; results replicated twice and then pooled) (*A* and *B*) and mRNA expression levels of desmin2 and *MYH2* normalized to *TBP* (desmin2: n = 8 for all groups; MYH2: n = 8 for control, n = 7 for WT-ADAMTS9 and mut-ADAMTS9) (*D*). *C*: Mouse TA muscles overexpressing ADAMTS9 or control plasmid were isolated at 10 weeks of age and used for Western blot analysis (n = 12 for each group). Statistical significance was determined using one-way ANOVA with Tukey test for multiple comparisons (*A*, *B*, and *D*) or paired Student t test (*C*). $^*P < 0.05$, $^{**}P < 0.01$ for genotype effect. A.U., arbitrary units.

seemed to be responsible for the decreased mitochondrial density because the level of *PGC-1α* and the protein levels of the mitochondrial complexes were partly rescued by the catalytically defective mut-ADAMTS9 (Fig. 5*F* and *G* and Supplementary Fig. 3*A* and *C–E*). The impaired mitochondrial biogenesis and dynamics may explain the lower density and the more-fragmented mitochondria observed when overexpressing ADAMTS9. Taken together, these results suggest that ADAMTS9 overexpression in skeletal muscle impairs mitochondrial function by disturbing mitochondrial respiration, biogenesis, and dynamics.

In human skeletal muscle from the Danish nondiabetic twin cohort, the C risk allele also was associated with decreased expression of mitochondrial electron transport complex subunits (Supplementary Table 3). Both CI and CIII subunits were significantly decreased (Fig. 5*H* and *I* and Supplementary Table 3). Furthermore, individuals carrying the C risk allele displayed decreased expression of the mitochondrial biogenesis enzyme *PGC-1α* (Fig. 5*J* and Supplementary Table 3). Altogether, the human data indicate that the rs4607103 C risk allele is associated with impaired insulin sensitivity and decreased expression of mitochondrial oxidative phosphorylation genes and *PGC-1α* in skeletal muscle.

ADAMTS9 Overexpression in Skeletal Muscle Alters the Metabolic Status

Untargeted metabolic characterization was performed on mouse skeletal muscle overexpressing ADAMTS9 or control plasmid to understand the impact of decreased mitochondrial function on metabolic alterations in glucose and lipid metabolism (Supplementary Fig. 4*A* and *B*). ATP levels were lower, whereas AMP levels were significantly higher, in skeletal muscle overexpressing ADAMTS9 compared with control plasmid (Fig. 6*A*), suggesting an energy-deficient state. In accordance with the high AMP/ATP ratio, phosphorylation level of Thr172 AMPK was increased (Fig. 6*B* and Supplementary Fig. 4*C*), and the internal stores of muscle glycogen were reduced (Fig. 6*C*).

Increased activity of pyruvate dehydrogenase, as indicated by decreased S293 phosphorylation (Fig. 6*D*), as well as decreased levels of phosphorylated hexose (Fig. 6*E*), suggest an increased rate of glycolysis. However, the pyruvate produced through glycolysis did not cause accumulation of lactate in ADAMTS9-overexpressing muscle (Supplementary Fig. 4*D*), potentially as a result of enhanced transport of lactate out of the cell, as *MCT1* and

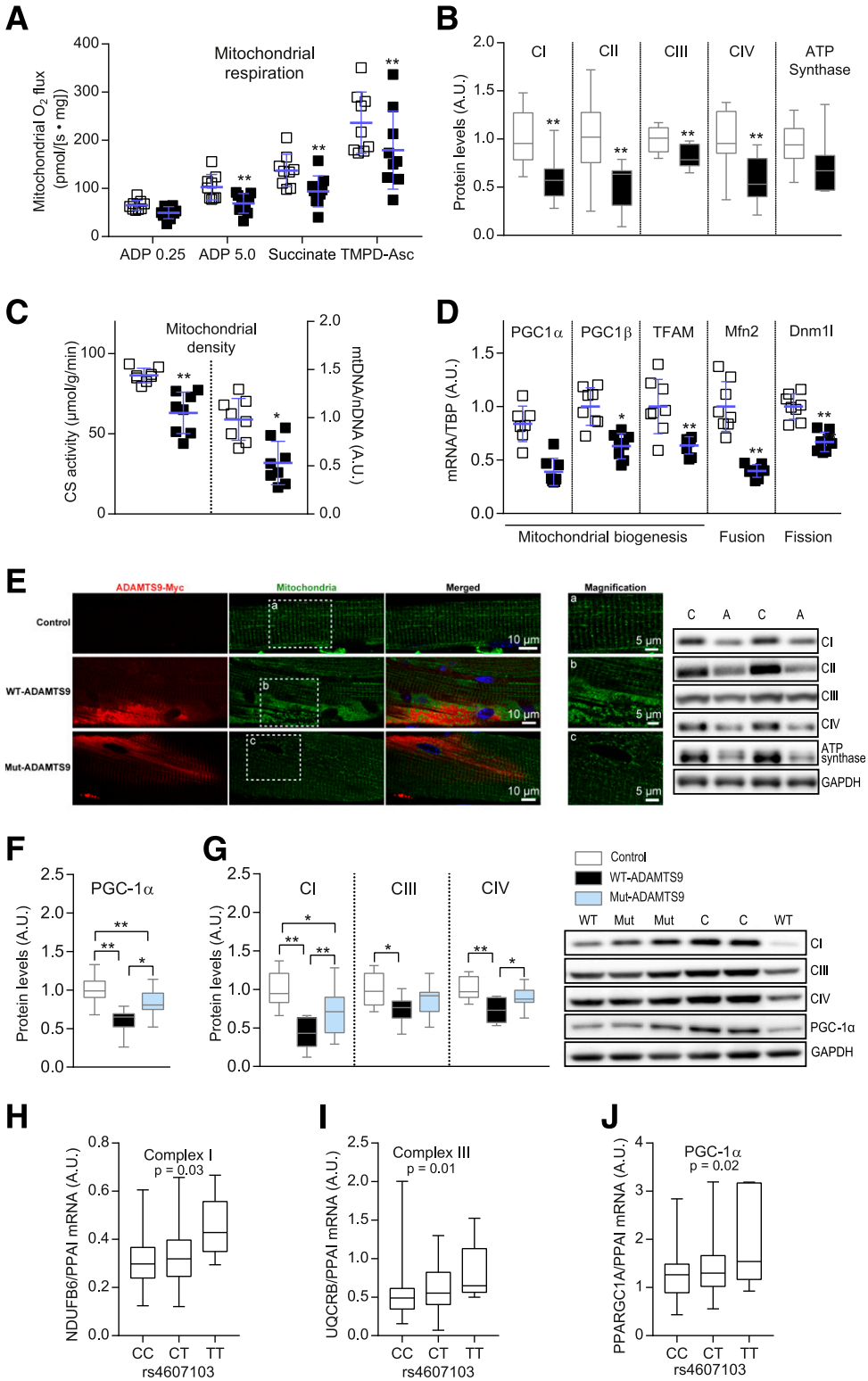

Figure 5—High *ADAMTS9* expression induces mitochondrial changes in mouse and human skeletal muscles. *A–D*: Mouse TA muscles overexpressing ADAMTS9 or control plasmid were isolated at 10 weeks of age and used for the following. *A*: Mitochondrial respiration (four replicates for each muscle, $n = 9$ for each group) normalized to citrate synthase (CS) activity. *B*: Western blot analysis (CI–CIV: $n = 12$ for each group; ATP synthase: $n = 11$ for each group; results replicated twice and pooled). *C*: Mitochondrial density determined by CS activity measurements and mitochondrial DNA (mtDNA) normalized to nDNA ($n = 8$ for each group). *D*: mRNA expression levels normalized to *TBP* ($n = 8$ for each group). *E–G*: Mouse TA muscles overexpressing WT-ADAMTS9, mut-ADAMTS9, or control plasmid. *E*: Immunohistochemistry (representative pictures [$n = 2$] double stained for myc-tag [ADAMTS9] [red] and mitochondrial CIV [green]; nuclei visualized using Hoechst stain [blue]). *F* and *G*: Western blot analysis ($n = 13$ for WT-ADAMTS9 and control, $n = 14$ for mut-ADAMTS9; results replicated twice and pooled). Statistical significance was determined using paired two-way ANOVA with Sidak test for multiple comparisons with repeated

MCT4 mRNA expression levels were increased (Fig. 6*F*). Of note, mRNA expression levels of the fatty acid oxidation proteins *Acadm*, *Acadl*, and *Acadvl* were reduced, suggesting that the capacity for fatty acid oxidation was downregulated in muscles overexpressing ADAMTS9 (Fig. 6*G*). Lipid accumulation in muscle as TAG was not affected by the presence of ADAMTS9 overexpression (Fig. 6*H*). The untargeted metabolomics analysis revealed that DAGs generally were increased. Because it has been shown in both mouse and human skeletal muscle that not all the various isomers of DAG influence insulin signaling (33,43), we studied these isomeric forms. We found the *sn*-1,2 isomer of DAG, which is known to inhibit insulin signaling through activation of protein kinase C (44), to be increased (Fig. 6*I*). In addition, it has been suggested that the accumulation of glycerophospholipids is important for the development of insulin resistance in skeletal muscle (45). We observed an increased level of phosphatidylcholine after ADAMTS9 overexpression (Fig. 6*J*). These data suggest that the defects in mitochondrial respiration may lead to reduced free fatty acid oxidation and thus accumulation of lipid intermediates.

DISCUSSION

In the current study, we substantiate that the rs4607103 C risk allele located 38 kilobases upstream of *ADAMTS9* is associated with insulin resistance and demonstrate that carriers of the C risk allele have elevated *ADAMTS9* expression in human skeletal muscle. Furthermore, we show that the C risk allele is associated with decreased insulin signaling and mitochondrial gene expression in human skeletal muscle tissue, which may explain the observed impairment in insulin sensitivity. These findings suggest that *ADAMTS9* is the gene responsible for the observed effect of the rs4607103 C risk allele in humans.

To evaluate the impact of ADAMTS9 on glucose homeostasis, we developed skeletal muscle–specific *Adamts9* KO mice. These mice were able to maintain similar plasma glucose levels as littermate controls with a significantly lower plasma insulin level, indicating improved insulin sensitivity. Furthermore, the enhanced insulin sensitivity in the muscle-specific *Adamts9* KO mice was substantiated by increased GIR and whole-body R_d as measured by hyperinsulinemic-euglycemic clamp in these mice. Collectively, these results indicate that KO of *Adamts9* specifically in skeletal muscle increases insulin sensitivity.

Overexpression of ADAMTS9 in TA muscle showed that ADAMTS9 negatively regulated the insulin signaling cascade, capillary density, cytoskeletal organization, and mitochondrial function in mouse skeletal muscle and resulted in accumulation of lipid intermediates, potentially caused by the defective mitochondrial function (46). Results from mice overexpressing ADAMTS9 further suggested that regulation of insulin sensitivity and insulin signaling was achieved through cleavage of ECM molecules and subsequent modulation of integrin receptor signaling.

The demonstration that ADAMTS9-mediated proteolysis of ECM components induce changes in muscle-specific insulin sensitivity is in line with other observations (8,10,11,14,16,17,47). However, the mechanistic link between altered integrin receptor signaling and insulin signaling remains to be established. Increased levels of ILK in ADAMTS9-overexpressing muscles may partially explain the observed attenuation of the insulin response, as it has recently been demonstrated that HFD-treated muscle-specific ILK KO mice have improved insulin sensitivity compared with control mice together with an increased capillary density (16). Similarly, FAK has been shown both in vitro and in vivo to regulate insulin sensitivity and the levels of mitochondria complexes in skeletal muscles (14,15,48). Furthermore, depletion of FAK has been shown to decrease angiogenesis (49).

The link between altered integrin receptor activity and impaired insulin sensitivity as well as mitochondrial function could potentially be explained by modulation of the cytoskeleton. Integrin receptor activity regulates the cytoskeleton, and cytoskeleton proteins, such as desmin, have been shown to be important for mitochondrial integrity and function (15,50). We found that in mice, ADAMTS9 overexpression decreases expression levels of desmin, which may suggest that ADAMTS9 regulates insulin signaling and mitochondrial function through cytoskeleton modulations.

In conclusion, the current study provides evidence that *ADAMTS9* is the responsible gene for the association between the rs4607103 C allele and insulin resistance in humans. Human skeletal muscle from individuals carrying the C risk allele displays both decreased insulin signaling and increased expression levels of *ADAMTS9*. Importantly, results from KO and overexpression of *Adamts9* in mouse skeletal muscle indicate that ADAMTS9 can regulate skeletal muscle insulin sensitivity. We identified possible molecular pathways that link ADAMTS9 to insulin signaling and propose a potential working mechanism (Fig. 6*K*). The data suggest a model in which a higher expression level of ADAMTS9 in skeletal muscle alters integrin signaling through proteolysis of the ECM, leading to decreased capillary density and insulin signaling as well as disturbed cytoskeleton organization. The disturbed cytoskeleton affects the mitochondria negatively, leading to decreased

measures (*A*), paired Student *t* test (*B–D*), or one-way ANOVA with Tukey test for multiple comparisons (*F* and *G*). Scatter plot data are mean ± SD. $^*P < 0.05$, $^{**}P < 0.01$ for genotype effect. *H–J*: C allele = rs4607103 risk allele; T allele = other allele. Danish nondiabetic twin cohort divided into genotypes (CC $n = 92$, CT $n = 58$, or TT $n = 6$). CI subunit *NDUFB6* (basal level; $P = 0.03$) (*H*), CIII subunit *UQCRB* (insulin stimulation; $P = 0.01$) (*I*), and *PGC-1α* (insulin stimulation; $P = 0.02$) (*J*). A mixed linear model was used, assuming an additive genetic effect. *P* values adjusted for sex, age, BMI, and family relationship. A.U., arbitrary units.

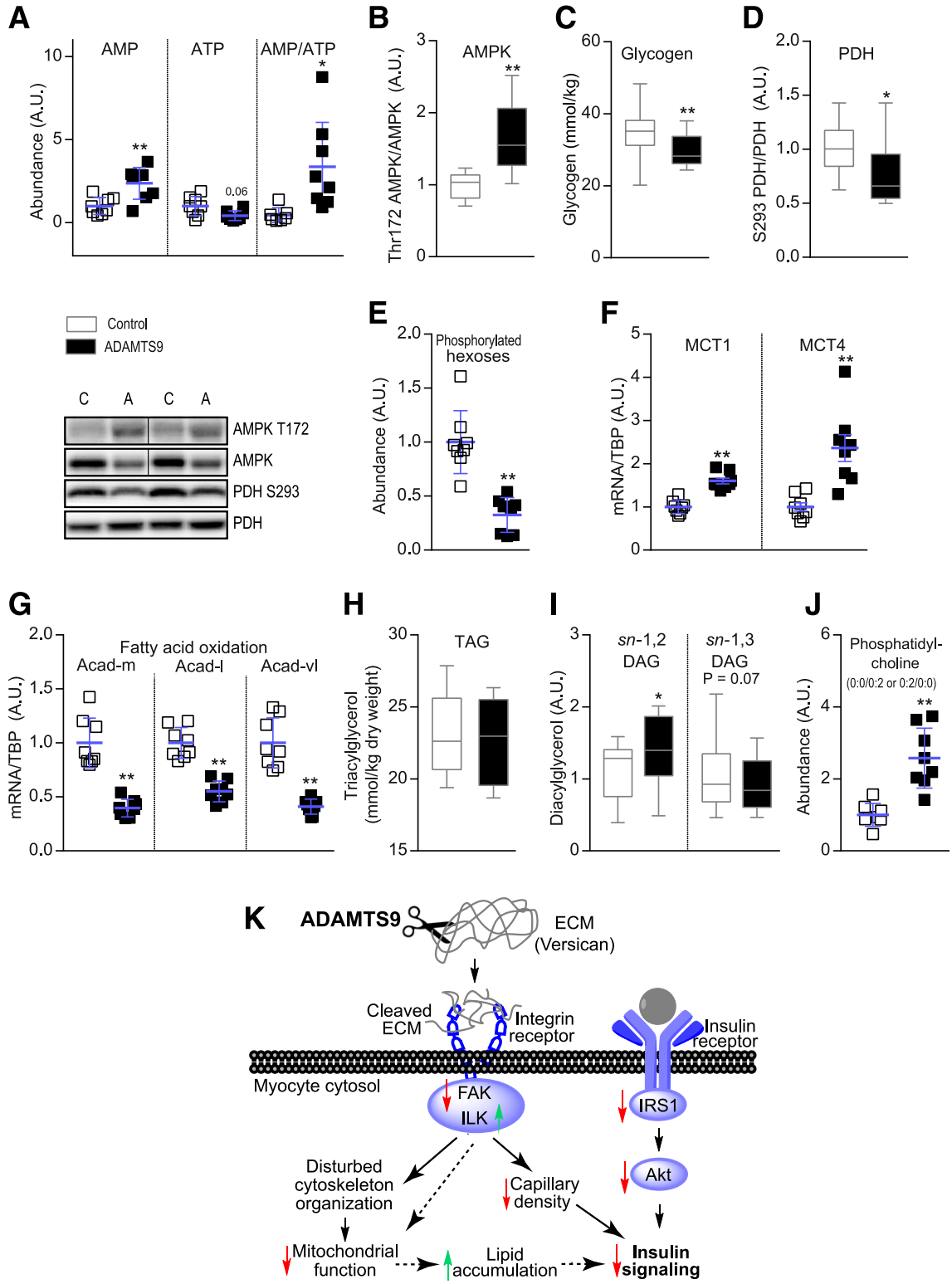

Figure 6—ADAMTS9 overexpression alters the metabolic status of muscles. *A*, *E*, and *J*: Mouse TA muscles overexpressing ADAMTS9 or control plasmid were isolated at 10 weeks of age and used for metabolomic analysis (n = 8 for each group) as follows: AMP and ATP (*A*), phosphorylated hexoses (*E*), and phosphatidylcholine (0:0/0:2 or 0:2/0:0) (*J*). *B* and *D*: Western blot analyses (n = 12 for each group; results replicated twice and then pooled). *C*: Glycogen measurements (n = 16 for each group). *F* and *G*: mRNA expression normalized to *TBP* (n = 8 for each group). *H*: Intramuscular TAG analysis (n = 12 for each group). *I*: DAG isomers *sn*-1,2 and *sn*-1,3 (n = 12 for each group, except for n = 11 for control *sn*-1,2 DAG). Statistical significance was determined using paired Student t test. Scatter plot data are mean ± SD. *$P < 0.05$, **$P < 0.01$ for effect of ADAMTS9 overexpression vs. control plasmid. Dividing lines have been used in some representative plots. *K*: Proposed mechanism for how high ADAMTS9 expression induces insulin resistance. See Discussion for details. A.U., arbitrary units.

oxidation of substrates and accumulation of lipids. Accumulation of lipid, disturbance of insulin signaling, and decreased capillary density together promote insulin resistance (Fig. 6*K*). Finally, we suggest that ADAMTS9 blockers may provide a novel therapeutic approach to treat type 2 diabetes–associated insulin resistance.

Acknowledgments. The authors thank L.M. Petersen (Novo Nordisk Foundation Center for Basic Metabolic Research) for excellent assistance with the mouse-related experiments; A. Bjerregaard, A. Forman, T. Lorentzen, and G. Klavsen (Novo Nordisk Foundation Center for Basic Metabolic Research) for technical assistance; M.M. Andersen, A. Munk, and L. Larsson (Novo Nordisk Foundation Center for Basic Metabolic Research) for assistance with glucose uptake studies in mice; and P. Sandbeck, G. Lademann, and T. Toldsted (Novo Nordisk Foundation Center for Basic Metabolic Research) for management assistance.

Funding. The study is part of the research activities in TARGET (The Impact of Our Genomes on Individual Treatment Response in Obese Children [www.target.ku.dk]) and BIOCHILD (Genetics and Systems Biology of Childhood Obesity in India and Denmark [www.biochild.ku.dk]). The study was supported by Novo Nordisk Foundation grants NNF10CC1016515 (to J.T.T.) and NNF14OC0009315, Innovation Fund Denmark grant 0603-00484, Danish Council for Independent Research grant DFF-4004-00235 (to J.T.T.), and National Institutes of Health grant HL-107147 (to S.S.A.). The Novo Nordisk Foundation Center for Basic Metabolic Research is an independent Research Center at the University of Copenhagen partially funded by an unrestricted donation from the Novo Nordisk Foundation (www.metabol.ku.dk).

The results and views expressed in the study represent those of the authors and not necessarily those of the Swedish Medical Products Agency, at which B.Z. is employed. B.Z. has not received any grants or any financial support from any sponsor for the present work.

Duality of Interest. No potential conflicts of interest relevant to this article were reported.

Author Contributions. A.-S.G., N.G., R.R.-M., S.H.L., T.B., H.S., A.F., N.W., K.S., M.K., M.B.B., S.C., C.P., A.K.S., J.B.B., J.D., L.G., S.G.V., A.N., B.K., J.F.P.W., S.L., S.S.A., H.-U.H., A.V., B.Z., O.P., J.T.T., T.H., and B.H. edited, revised, and approved the final manuscript. A.-S.G., N.G., R.R.-M, J.T.T., T.H., and B.H. contributed to the overall interpretation of results. A.-S.G., S.H.L., N.W., M.K., J.D., A.N., S.S.A., J.T.T., and B.H. designed the mouse KO model. A.S.-G., S.H.L., N.W., M.K., M.B.B., S.C., and J.D. performed experiments and analyzed data of the mouse KO model. A.-S.G., S.H.L., K.S., C.P., A.K.S., S.G.V., B.K., S.L., S.S.A., J.T.T., and B.H. designed the mouse overexpression model. A.-S.G., S.H.L., K.S., M.B.B., A.K.S., J.D., S.L., and J.T.T. performed experiments and analyzed data of the mouse overexpression model. A.-S.G. and B.H. drafted the manuscript. N.G., R.R.-M., T.B., H.S., A.F., J.B.B., L.G., J.F.P.W., H.-U.H., A.V., B.Z., O.P., and T.H. designed the human samples model. N.G., R.R.-M., T.B., H.S., A.F., J.B.B., L.G., H.-U.H., and B.Z. performed the experiments and analyzed data of the human samples model. T.H. and B.H. are the guarantors of this work and, as such, had full access to all the data in the study and take responsibility for the integrity of the data and the accuracy of the data analysis.

References

1. Hara K, Kadowaki T, Odawara M. Genes associated with diabetes: potential for novel therapeutic targets? Expert Opin Ther Targets 2016;20:255–267

2. Grarup N, Sandholt CH, Hansen T, Pedersen O. Genetic susceptibility to type 2 diabetes and obesity: from genome-wide association studies to rare variants and beyond. Diabetologia 2014;57:1528–1541

3. Zeggini E, Scott LJ, Saxena R, et al.; Wellcome Trust Case Control Consortium. Meta-analysis of genome-wide association data and large-scale replication identifies additional susceptibility loci for type 2 diabetes. Nat Genet 2008;40:638–645

4. Trombetta M, Bonetti S, Boselli ML, et al. PPARG2 Pro12Ala and ADAMTS9 rs4607103 as "insulin resistance loci" and "insulin secretion loci" in Italian individuals. The GENFIEV study and the Verona Newly Diagnosed Type 2 Diabetes Study (VNDS) 4. Acta Diabetol 2013;50:401–408

5. Boesgaard TW, Gjesing AP, Grarup N, et al.; EUGENE2 Consortium. Variant near ADAMTS9 known to associate with type 2 diabetes is related to insulin resistance in offspring of type 2 diabetes patients–EUGENE2 study. PLoS One 2009;4:e7236

6. Somerville RP, Longpre J-M, Jungers KA, et al. Characterization of ADAMTS-9 and ADAMTS-20 as a distinct ADAMTS subfamily related to Caenorhabditis elegans GON-1. J Biol Chem 2003;278:9503–9513

7. Tharmarajah G, Eckhard U, Jain F, et al. Melanocyte development in the mouse tail epidermis requires the Adamts9 metalloproteinase. Pigment Cell Melanoma Res 2018;31:693–707

8. Williams AS, Kang L, Wasserman DH. The extracellular matrix and insulin resistance. Trends Endocrinol Metab 2015;26:357–366

9. Berria R, Wang L, Richardson DK, et al. Increased collagen content in insulin-resistant skeletal muscle. Am J Physiol Endocrinol Metab 2006;290:E560–E565

10. Kang L, Ayala JE, Lee-Young RS, et al. Diet-induced muscle insulin resistance is associated with extracellular matrix remodeling and interaction with integrin alpha2beta1 in mice. Diabetes 2011;60:416–426

11. Kang L, Lantier L, Kennedy A, et al. Hyaluronan accumulates with high-fat feeding and contributes to insulin resistance. Diabetes 2013;62:1888–1896

12. Irwin WA, Bergamin N, Sabatelli P, et al. Mitochondrial dysfunction and apoptosis in myopathic mice with collagen VI deficiency. Nat Genet 2003;35:367–371

13. Werner E, Werb Z. Integrins engage mitochondrial function for signal transduction by a mechanism dependent on Rho GTPases. J Cell Biol 2002;158:357–368

14. Bisht B, Srinivasan K, Dey CS. In vivo inhibition of focal adhesion kinase causes insulin resistance. J Physiol 2008;586:3825–3837

15. Huang D, Khoe M, Ilic D, Bryer-Ash M. Reduced expression of focal adhesion kinase disrupts insulin action in skeletal muscle cells. Endocrinology 2006;147:3333–3343

16. Kang L, Mokshagundam S, Reuter B, et al. Integrin-linked kinase in muscle is necessary for the development of insulin resistance in diet-induced obese mice. Diabetes 2016;65:1590–1600

17. Zong H, Bastie CC, Xu J, et al. Insulin resistance in striated muscle-specific integrin receptor beta1-deficient mice. J Biol Chem 2009;284:4679–4688

18. Zethelius B, Lithell H, Hales CN, Berne C. Insulin sensitivity, proinsulin and insulin as predictors of coronary heart disease. A population-based 10-year, follow-up study in 70-year old men using the euglycaemic insulin clamp. Diabetologia 2005;48:862–867

19. Clausen JO, Borch-Johnsen K, Ibsen H, et al. Insulin sensitivity index, acute insulin response, and glucose effectiveness in a population-based sample of 380 young healthy Caucasians. Analysis of the impact of gender, body fat, physical fitness, and life-style factors. J Clin Invest 1996;98:1195–1209

20. Poulsen P, Levin K, Petersen I, Christensen K, Beck-Nielsen H, Vaag A. Heritability of insulin secretion, peripheral and hepatic insulin action, and intracellular glucose partitioning in young and old Danish twins. Diabetes 2005;54:275–283

21. Gillberg L, Jacobsen SC, Ribel-Madsen R, et al. Does DNA methylation of PPARGC1A influence insulin action in first degree relatives of patients with type 2 diabetes? [published correction appears in PLoS One 2013;8]. PLoS One 2013;8:e58384

22. Staiger H, Machicao F, Kantartzis K, et al. Novel meta-analysis-derived type 2 diabetes risk loci do not determine prediabetic phenotypes. PLoS One 2008;3:e3019

23. Koo B-H, Coe DM, Dixon LJ, et al. ADAMTS9 is a cell-autonomously acting, anti-angiogenic metalloprotease expressed by microvascular endothelial cells. Am J Pathol 2010;176:1494–1504

24. Dubail J, Aramaki-Hattori N, Bader HL, et al. A new Adamts9 conditional mouse allele identifies its non-redundant role in interdigital web regression. Genesis 2014;52:702–712

25. Schwander M, Leu M, Stumm M, et al. Beta1 integrins regulate myoblast fusion and sarcomere assembly. Dev Cell 2003;4:673–685
26. Agerholm M, Dall M, Jensen BAH, et al. Perturbations of NAD+ salvage systems impact mitochondrial function and energy homeostasis in mouse myoblasts and intact skeletal muscle. Am J Physiol Endocrinol Metab 2018;314:E377–E395
27. Livak KJ, Schmittgen TD. Analysis of relative gene expression data using real-time quantitative PCR and the 2(-Delta C(T)) method. Methods 2001;25:402–408
28. Larsen S, Danielsen JH, Søndergård SD, et al. The effect of high-intensity training on mitochondrial fat oxidation in skeletal muscle and subcutaneous adipose tissue. Scand J Med Sci Sports 2015;25:e59–e69
29. Boushel R, Gnaiger E, Schjerling P, Skovbro M, Kraunsøe R, Dela F. Patients with type 2 diabetes have normal mitochondrial function in skeletal muscle. Diabetologia 2007;50:790–796
30. McCulloch DR, Le Goff C, Bhatt S, Dixon LJ, Sandy JD, Apte SS. Adamts5, the gene encoding a proteoglycan-degrading metalloprotease, is expressed by specific cell lineages during mouse embryonic development and in adult tissues. Gene Expr Patterns 2009;9:314–323
31. Dahl R, Larsen S, Dohlmann TL, et al. Three-dimensional reconstruction of the human skeletal muscle mitochondrial network as a tool to assess mitochondrial content and structural organization. Acta Physiol (Oxf) 2015;213:145–155
32. Steffensen CH, Roepstorff C, Madsen M, Kiens B. Myocellular triacylglycerol breakdown in females but not in males during exercise. Am J Physiol Endocrinol Metab 2002;282:E634–E642
33. Serup AK, Alsted TJ, Jordy AB, Schjerling P, Holm C, Kiens B. Partial disruption of lipolysis increases postexercise insulin sensitivity in skeletal muscle despite accumulation of DAG. Diabetes 2016;65:2932–2942
34. Dall M, Penke M, Sulek K, et al. Hepatic NAD^+ levels and NAMPT abundance are unaffected during prolonged high-fat diet consumption in C57BL/6JBomTac mice. Mol Cell Endocrinol 2018;473:245–256
35. Petersen PS, Jin C, Madsen AN, et al. Deficiency of the GPR39 receptor is associated with obesity and altered adipocyte metabolism. FASEB J 2011;25:3803–3814
36. Parlevliet ET, de Leeuw van Weenen JE, Romijn JA, Pijl H. GLP-1 treatment reduces endogenous insulin resistance via activation of central GLP-1 receptors in mice fed a high-fat diet. Am J Physiol Endocrinol Metab 2010;299:E318–E324
37. Enomoto H, Nelson CM, Somerville RP, et al. Cooperation of two ADAMTS metalloproteases in closure of the mouse palate identifies a requirement for versican proteolysis in regulating palatal mesenchyme proliferation. Development 2010;137:4029–4038
38. Flannery CR, Zeng W, Corcoran C, et al. Autocatalytic cleavage of ADAMTS-4 (Aggrecanase-1) reveals multiple glycosaminoglycan-binding sites. J Biol Chem 2002;277:42775–42780
39. Nandadasa S, Foulcer S, Apte SS. The multiple, complex roles of versican and its proteolytic turnover by ADAMTS proteases during embryogenesis. Matrix Biol 2014;35:34–41
40. Delcommenne M, Streuli CH. Control of integrin expression by extracellular matrix. J Biol Chem 1995;270:26794–26801
41. Mathew R. Pathogenesis of pulmonary hypertension: a case for caveolin-1 and cell membrane integrity. Am J Physiol Heart Circ Physiol 2014;306:H15–H25
42. Winter L, Wittig I, Peeva V, et al. Mutant desmin substantially perturbs mitochondrial morphology, function and maintenance in skeletal muscle tissue. Acta Neuropathol 2016;132:453–473
43. Lundsgaard A-M, Sjøberg KA, Høeg LD, et al. Opposite regulation of insulin sensitivity by dietary lipid versus carbohydrate excess. Diabetes 2017;66:2583–2595
44. Finck BN, Hall AM. Does diacylglycerol accumulation in fatty liver disease cause hepatic insulin resistance? BioMed Res Int 2015;2015:104132
45. Meikle PJ, Summers SA. Sphingolipids and phospholipids in insulin resistance and related metabolic disorders. Nat Rev Endocrinol 2017;13:79–91
46. Camporez JP, Wang Y, Faarkrog K, Chukijrungroat N, Petersen KF, Shulman GI. Mechanism by which arylamine *N*-acetyltransferase 1 ablation causes insulin resistance in mice. Proc Natl Acad Sci U S A 2017;114:E11285–E11292
47. Kang L, Mayes WH, James FD, Bracy DP, Wasserman DH. Matrix metalloproteinase 9 opposes diet-induced muscle insulin resistance in mice. Diabetologia 2014;57:603–613
48. Durieux A-C, D'Antona G, Desplanches D, et al. Focal adhesion kinase is a load-dependent governor of the slow contractile and oxidative muscle phenotype. J Physiol 2009;587:3703–3717
49. Wary KK, Kohler EE, Chatterjee I. Focal adhesion kinase regulation of neovascularization. Microvasc Res 2012;83:64–70
50. Milner DJ, Mavroidis M, Weisleder N, Capetanaki Y. Desmin cytoskeleton linked to muscle mitochondrial distribution and respiratory function. J Cell Biol 2000;150:1283–1298